PULSATIONS IN THE SEPARATION ZONE OF A FREE CAVERN AT A SUPERSONIC STREAM VELOCITY

V. I. Zapryagaev

UDC 534.132:532.526.5:533.6.011.5

The stationary flow structure in the domain between two bodies, one of which is in the other's wake, was examined in [1, 2]. According to [3], such a configuration of the separation domain is classified as a free cavern. Assumption about the nature of pulsation phenomena in flows of such type can be made by an analogy between the flow in a free cavern and the pulsations in channels which are considered in both axisymmetric [4, 5] and plane models [6-9] for a different external flow velocity. Theoretical investigations of pulsation phenomena in cavities based on using phase relationships for acoustic waves in the cavity and waves being propagated in a shear layer are presented in [5, 10, 11]. In a linear formulation the problem of pulsation excitation in a rectangular cavity is solved for subsonic flows by using the results of computing the shear layer stability [12]. The solution of the problem of pulsations in cavity with a supersonic flow velocity is presented in [11] in a two-dimensional formulation by the numerical solution of the Navier–Stokes equations.

Results of an experimental investigation of pressure fluctuations in an axisymmetric free cavern for a stream Mach number of $M_\infty = 2.05$ are shown in this paper. Two characteristic types of fluctuations (high-frequency and low-frequency) were observed depending on the geometric parameters of the model. The physical pattern of the high-frequency fluctuation phenomena is illustrated by a linear one-dimensional theory, which permits evaluation of the value of the natural fluctuation frequencies.

1. The experimental investigation was performed in a T-333 wind tunnel whose metrological characteristics are presented in [13]. The model diagram is shown in Fig. 1, where 1 is a steel cone with 10° half-angle fastened in a rhomboidal holder with d = 40 mm diameter of the base section, 2 are flat interchangeable obstacles with the relative diameter D/d = 1.0, 1.28, 2.0 which are arranged coaxially with the cone, and 3 is the piezosensor LKh-601 for the pressure fluctuations that is mounted in the center of the obstacle. The distance ℓ from the bottom section to the obstacle varied in the range $\bar{\ell} = 2\ell/d = 0.1\text{-}5.0$ because of displacement of the obstacle.

The investigation was conducted for the following flow parameters: $M_\infty = 2.05$, Reynolds number calculated according to the diameter of the cone base section $Re_d = 1.71 \cdot 10^6$, stream stagnation temperature $T_0 = 261°K$, static free-stream pressure $p_\infty = 0.343 \cdot 10^5$ N/m^2. The nonuniformity of the Mach number field is <1% [13]. The Reynolds number along the cone length is $4.84 \cdot 10^6$ which is greater than the critical value at which the transition from a laminar into a turbulent boundary layer would occur ($Re^* \cong 3 \cdot 10^6$ [14]). This permits considering the boundary layer on the cone turbulent near the endface.

The range of frequencies being measured for the LKh-601 piezosensor with a preamplifier is 0.02-20 kHz. The piezosensor was calibrated by a PP-101 piston-phone before and after the experiment. The signal from the fluctuation sensor went to the input of a "Tembr-2" magnetic tape recorder and was inscribed on magnetic tape. During processing the magnetic tape recorder signal was delivered to a one-third octave RFT-01004 analyzer which was used to perform a spectrum analysis in the 20-1000 Hz frequency range. Analysis of the frequency spectrum in the 1-20 kHz band was performed by a S5-3 heterodyne type analyzer with 200-Hz bandwidth, which operated in combination with a N-110 recorder. The magnetic tape recorder amplitude–frequency characteristic (AFC) was taken into account by inserting appropriate corrections into the measured spectrum of the signal being investigated. The accuracy of the fluctuation amplitude measurements is estimated at 2 dB and of the frequency is 4%.

To verify the piezosensor response to vibrations, a recording was made in one of the regimes, of the vibration signal from the piezosensor whose membrane is isolated from the action of the pressure fluctuation. Comparing the spectral composition of the vibration

Novosibirsk. Translated from Zhurnal Prikladnoi Mekhaniki i Tekhnicheskoi Fiziki, No. 6, pp. 50-58, November-December, 1985. Original article submitted August 29, 1984.

0021-8944/85/2606-0802$09.50

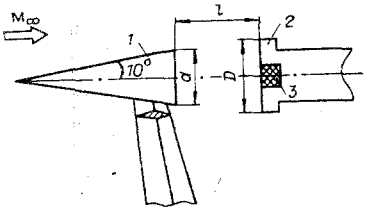

Fig. 1

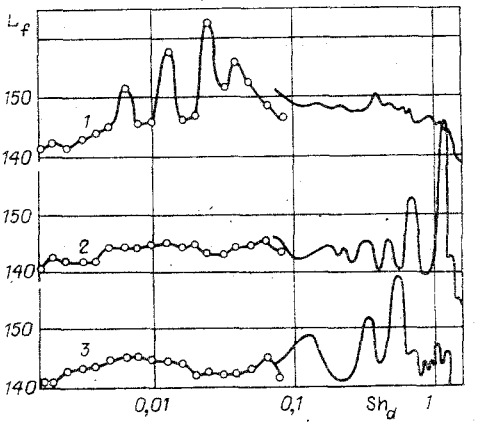

Fig. 2

signal and a signal due to presure fluctuations in the presence of a parasitic vibration signal showed that the magnitude of the vibration signal is approximately an order of magnitude less than the useful signal in the whole frequency band under investigation. The streamlining process was photographed by a IAB-451 shadowgraph device by using a spark light source with $\sim 10^{-6}$ sec exposure. The Schlieren photographs were obtained by using a diaphragm-annular knife system, which permitted visualization of the optical inhomogeneity gradient in all directions.

2. The spectral comosition of pressure fluctuations is represented in Fig. 2 for $\bar{D} = 1.28$ for a different obstacle position: lines 1-3 corresponds to $\bar{\ell} = 0.4$; 0.72; 1.45. The fluctuation level at the frequency f, defined as $L_f = 20 \log(p_f/p_{00})$, where p_f is the amplitude of the pressure fluctuations at the frequency f in the frequency band being measured, and $p_{00} = 2 \cdot 10^{-5}$ N/m^2, is plotted along the ordinate axis. In this case the Strouhal number was calculated with respect to the diameter of the cone base section and the free stream velocity U_∞: $Sh_d = (fd)/U_\infty$. A characteristic feature of the pressure fluctuation spectrum is the presence of peaks in the discrete components whose magnitude reaches 166 dB, which is more than 20 dB above the magnitude of the background fluctuations in the working part of the apparatus. The Schlieren photographs of the flow are represented for $\bar{D} = 1.28$ in Fig. 3 for several values of the relative distance: a-d correspond to $\bar{\ell} = 0.4$; 0.4; 0.72; 1.1.

Two kinds of fluctuations, differing substantially by the values of the discrete frequencies, are observed. There are fluctuations with Strouhal number $Sh_d \sim 1$ in almost all the modes investigated (see the dependence $L_f(Sh_d)$ for $\bar{\ell} = 0.72$; 1.45 in Fig. 2). Acoustic radiation from the cavern (see Fig. 3) is seen in the Schlieren photographs of the flow process. The absence of visible acoustic radiation in the lower part of the model is apparently explained by the destructive action of the pylon sustaining cone on the wave front of the acoustic radiation. Clearly seen in Fig. 3d are the wavy shape of the shear layer interacting with the edge of the obstacle, and the axial symmetry of the shear layer perturbation. The shear layer perturbation at a distance of approximately (1/3) ℓ from the obstacle has an external form that can be treated as a large-scale vortex or a coherent structure. The wavelength of the perturbation being propagated in the shear layer corresponds to the wavelength λ of the coherent structures in the jet, referred to the nozzle diameter d_c. The values of λ observed by different investigators are presented in [15] and are described well by the linear dependence $\lambda = 0.55 d_c$. The values of λ/d measured in the shear layer are taken approximately the same in this case. For instance, for $\bar{\ell} = 1.1$ $\lambda/d = 0.52$ (see Fig. 3).

Values of the frequency of the discrete tone are shown in Fig. 4, where the dependence $Sh_\ell = (f\ell)/U_\infty$ on the relative range $\bar{\ell} = 2\ell/d$ is presented with 1) $\bar{D} = 1.0$, 2) $\bar{D} = 1.28$, 3) data in [7], 4) results in [5]. The data from [5, 7] are taken for $M_\infty = 2.0$. The separation of all the frequencies into vibrations modes and the good agreement between the experimental values obtained in different papers are seen. Values on the graph are conditionally superposed for $\bar{\ell} = 5.0$ for the results of [5], as is considered possible since the dependence $Sh_\ell(\bar{\ell})$ vanishes as $\bar{\ell}$ increases. The data in [5] are obtained for both plane caverns and axisymmetric channels formed by the rectangular turning of a pointed cone. A plane cavern formed on the wall of a wind tunnel was investigated [7].

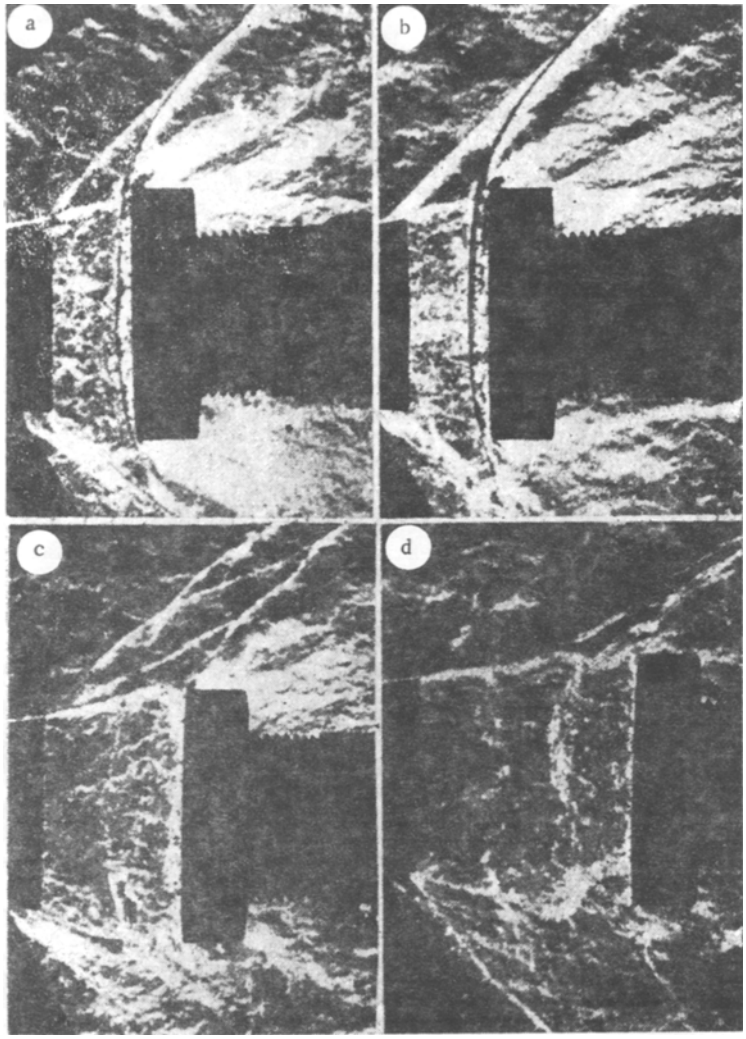

Fig. 3

The minimal values of Sh_ℓ for caverns are similar in order of magnitude to the natural acoustic vibrations frequencies in a half-open tube. For the longitudinal acoustic vibrations in a tube, one end of which is closed and the other open, $Sh_\ell = 0.25$; here the sound speed in the tube [16] is taken as the characteristic velocity. This comparison between the values of the natural vibrations frequencies in a cavity and the acoustic vibrations in a tube permits considering that the acoustic waves being propagated in a cavity play an important part in a vibrational process of this kind.

Low-frequency fluctuations are observed for small relative distances $\bar{\ell}$ and have the characteristic values $Sh_d \sim 0.01$ (see the spectrum 1 in Fig. 2, say). The pressure fluctuation level at the frequencies $Sh_\ell = 0.25\text{-}0.8$ ($Sh_\ell = \bar{\ell}\, Sh_d$) here exceeds the background by approximately 10 dB, but no discrete components are observed in this spectrum band. The low-frequency fluctuations are also characterized by several modes. The Schlieren photographs of the flow pattern corresponding to this mode are presented in Figs. 3a and b. Two photographs correspond to two realizations of the very same mode. The distinction between them is due to the phases of the vibrational process. The flow in Fig. 3a separated from the trailing edge, while it is seen in Fig. 3b that the separation point was shifted a distance 0.1d from the bottom edge to the cone generatrix. Shifting of the separation point S from the sharp trailing edge to the cone generatrix indicates that the pressure near the cone endface for this mode can be increased to a quantity which is greater than the drop without separation sustained by the boundary layer. For $\bar{D} = 2.0$ and $\bar{\ell} = 0.5$ the flow separation point is always on the cone generatrix, which is due to the large size of the obstacle. Processing the flow Schlieren photographs showed that the boundary layer separation

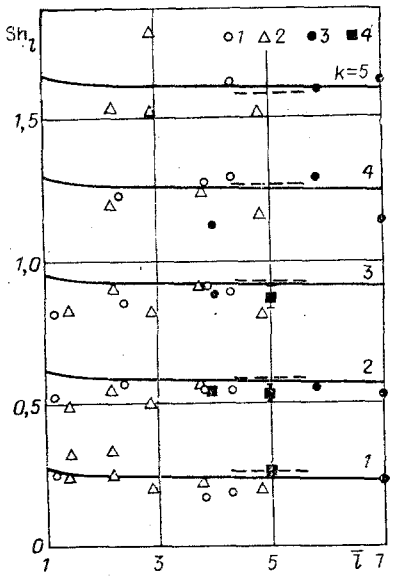

Fig. 4

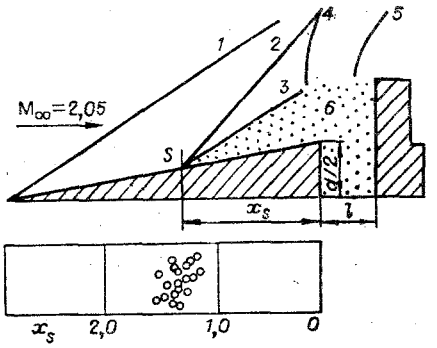

Fig. 5

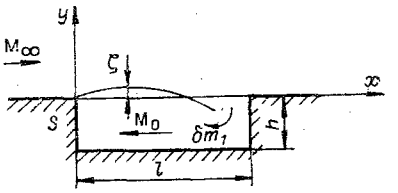

Fig. 6

point for several realizations is at a different distance from the bottom section x_s. The mean value of the distance x_s is 1.2d for $\bar{D} = 2.0$, $\bar{\ell} = 0.5$, while the span of the vibrations reaches 0.35d. The flow diagram for $\bar{D} = 2.0$, $\bar{\ell} = 0.5$ is shown in Fig. 5, where 1 is the attached bow compression shock, 2 is the compression shock associated with flow separation, 3 is the shear layer, 4 is the compression shock, 5 is the detached compression shock near the disc, and 6 is the separation domain. All the flow elements listed above, with the exception of the bow shock, are involved in the fluctuation process; for instance, values of x_s are superposed in the lower part of Fig. 5 for different realizations of the fluctuation process. The interval between realizations is 2-3 sec, while the characteristic frequencies of this process is ∿70 Hz; therefore, this graph illustrates only the location of the separation point x_s but not the dependence $x_s(t)$.

Fluctuations accompanying the displacement of the separation point are due to periodic influx of a certain mass of gas into the stagnation domain and efflux out, and are called delivery vibrations [17]. Vibrations of the separation domain with a substantial change in the shape of the latter are called a nonstationary mode of the second kind in [18]. The dimensionless fluctuation frequency for the mode of the second kind, calculated according to the stream velocity rather than according to the sound speed as was done in [18], takes on the minimal value 0.13 (0.009-0.051 in this paper, the disc diameter D is taken as characteristic dimension). The similarity of the low-frequency fluctuations described above to those kinds of vibrations mentioned in [17, 18] is based on frequency values that are close in order of magnitude and on substantial displacement of the separation point during the vibrational process. This similarity can apparently be a basis for assumptions on the similitude of these kinds of fluctuations.

3. The flow by a stream with $M_\infty > 1$ around a cavity is considered as the design model for high-frequency vibrations. The possibility of the existence of a reverse flow with $M_0 =$ const is assumed (it can reach the value 0.5, see [7], say). For definite relationships between the length ℓ, the depth h, and the thickness of the boundary layer in the cavity, intensive fluctuations occur. Acoustic waves, quite noticeable in the shadow photographs, are emitted here into the stream. The boundary layer being separated at the point S shapes a shear flow that vibrates near the middle position. Interaction between the vibration shear layer and the rear endface of the cavity causes a periodic influx and efflux of a certain mass of gas. The efflux of the gas from the cavity results in formation of perturbations in the boundary layer downstream of the rear endface [8]. Perturbations are propagated within the cavity from the rear to the forward endface (Fig. 6), reach it and are reflected, hence perturbing the shear layer near the point of separation S. The perturbation generated in the shear layer near the point S is washed downstream, reaches the rear endface of the cavity and interacts, consequently, a new portion of gas flows into the cavity (or flows out of the cavity). Interaction near the point of separation S causes a change in intensity of the perturbation that is propagated as a compression shock or a fan or rarefaction waves into the external stream.

The physical pattern elucidated for the fluctuation in the cavity is in agreement with [5, 10, 11] and permits a dispersion equation to be obtained. We assume that the perturbation being formed for $x = \ell$ during deflection of the shear layer near the rear endface, is propagated in the cavity in the form of a plane acoustic wave. We shall consider the interaction between acoustic waves in the cavity and the shear layer to be realized only near the endfaces. Let us note the analogy of the approach to the description of this phenomenon to the method of investigating the process of generating discrete tones by a supersonic underexpanded jet impinging on an obstacle [19].

Neglecting viscosity, heat conduction, and entropy changes, the longitudinal acoustic vibrations of the gas in the cavity are described by the following system

$$\frac{\partial \bar{v}}{\partial \tau} - M_0 \frac{\partial \bar{v}}{\partial \xi} + \frac{\partial \bar{p}}{\partial \xi} = 0, \quad \frac{\partial \bar{p}}{\partial \tau} - M_0 \frac{\partial \bar{p}}{\partial \xi} + \frac{\partial \bar{v}}{\partial \xi} = 0. \tag{3.1}$$

Here $\bar{p} = p'/\kappa p_0$, $\bar{v} = v'/a_0$ are dimensionless pressure and velocity perturbations, κ is the adiabatic index, p_0, a_0 is the average pressure and the sound speed in the cavity, $\xi = x/\ell$, $\tau = ta_0/\ell$ are the dimensionless coordinate and time, and ℓ is the length of the cavity. The solution of the system (3.1) is the superposition of waves in the form [20]

$$\begin{aligned} \bar{v} &= [A_v \varphi_1(\xi) + A_p \varphi_2(\xi)] \exp(\omega\tau), \\ \bar{p} &= [A_v \varphi_2(\xi) + A_p \varphi_1(\xi)] \exp(\omega\tau), \end{aligned} \tag{3.2}$$

where $\omega = \omega_r + i\omega_i$; A_p, A_v are constant coefficients

$$\varphi_1(\xi) = \frac{1}{2}\left[\exp\left(\frac{\omega\xi}{M_0 - 1}\right) + \exp\left(\frac{\omega\xi}{M_0 + 1}\right)\right];$$
$$\varphi_2(\xi) = \frac{1}{2}\left[\exp\left(\frac{\omega\xi}{M_0 - 1}\right) - \exp\left(\frac{\omega\xi}{M_0 + 1}\right)\right].$$

Deviation of the shear layer from its mean position will be described as

$$\zeta = C\xi \exp(\omega\tau - i\alpha\xi),$$

where $\zeta = y/\ell$ is the deflection, α is the wave number of the perturbations being propagated along the shear layer, and $C = \text{const}$. It is assumed that $\text{Im}\{\alpha\} = 0$. The linear form of perturbation growth in the shear layer can be considered as the first term in a series expansion of the standard exponential growth of the perturbations and since we are interested in the relatively small range ($\alpha\xi \sim 1$), then the mentioned expansion can be used for convenience in the calculations. Experimentally, such a growth of the vibrations in an axisymmetric jet is obtained in [21].

Near the forward wall of the cavern ($\xi = 0$) the acoustic vibration parameters are connected by the relationship

$$\bar{p}/\bar{v}|_{\xi=0} = Z, \tag{3.3}$$

where Z is the acoustic impedance of the forward wall, a complex number in the general case. Vibrations of the shear layer on the rear endface result in a periodic influx (efflux) of a certain mass of gas

$$\delta m_1 = F(\zeta) = -\int_{\zeta_0}^{\zeta} \rho_1(y)\, U(y)\, dy.$$

The minus sign is due to the selection of the direction ζ, for $(\zeta - \zeta_0) < 0$, $\delta m_1 > 0$ the gas flows into the cavity, ζ_0 is the coordinate of the separating streamline. For small boundary vibrations ($(\zeta - \zeta_0) \ll h/\ell$) the mass of gas transferred by longitudinal fluctuations into the cavity is determined from the continuity equation and equals

$$\delta m_0 = \rho_0 U_0 (\bar{p} - \bar{v}/M_0)\bar{h},$$

where $\bar{h} = h/\ell$ for the plane or $\bar{h} = D/4\ell$ for the axisymmetric case. Equating the masses of gas δm_1 and δm_0, we obtain the boundary condition on the cavity rear endface

$$\rho_0 U_0 (\bar{p} - \bar{v}/M_0)\bar{h}|_{\xi=1} = F(\zeta)|_{\xi=1}. \tag{3.4}$$

For small perturbations the relation between the angle of shear layer deflection and the pressure fluctuations is obtained by linearizing the relationship for an oblique compression shock or rarefaction wave and is given by the expression

$$\left.\frac{\partial\zeta}{\partial\xi}\right|_{\xi=0}=\left.\frac{\sqrt{M_\infty^2-1}}{M_\infty^2}e^{i\theta}\bar{p}\right|_{\xi=0}. \tag{3.5}$$

An analogous relation is obtained in [22], the difference is that the lag time θ expressing the phase shift between the pressure vibrations and the layer near the separation point is introduced in (3.5). This lag time is called the "delay time of vortex shedding."

Therefore, to solve the problem on the combined longitudinal vibrations of the gas in the cavity and the shear layer, it is necessary that the solution (3.2) satisfy the boundary conditions (3.3)-(3.5). We take the cavity forward wall to be acoustically hard

$$\bar{v}|_{\xi=0}=0 \quad (Z\to\infty).$$

This latter circumstance assumes the existence of a standing acoustic wave in the cavity. After appropriate manipulations, we obtain the dispersion equation

$$(M_0-1)\exp\left(\frac{\omega}{M_0-1}\right)+(M_0+1)\exp\left(\frac{\omega}{M_0+1}\right)=-R\exp[i(\theta-\alpha)], \tag{3.6}$$

where

$$R=2\frac{\rho_\infty a_\infty}{\rho_0 a_0}\frac{\sqrt{M_\infty^2-1}}{\bar{h}M_\infty^2}.$$

It is here assumed that the shear layer is a tangential discontinuity and $\zeta_0 = 0$, which yields

$$F(\zeta)=-\rho_\infty a_\infty M_\infty\zeta. \tag{3.7}$$

To solve the dispersion equation (3.6) it is necessary to know the dependence of the wave number of the perturbations being propagated in the shear layer on the frequency, and the value of the phase shift θ.

Data on the mode of the shear layer vibrations above the cavity mouth are obtained for the flow around a cavern in an experimental investigation of the shear layer [6], and it is found that the phase shift between the vibrations of the longitudinal velocity and the vibrations of the shear layers is $-\pi/2$. It is seen from the form of the solution (3.2) that the pressure vibrations and the velocity in the cavity are cophasal for $\xi = 0$. We use the value $\theta = -\pi/2$ in the subsequent calculations.

The wave number is often determined in terms of the convective velocity $\alpha = \omega/U_c$, whose value depends on the shear layer thickness, the flow velocity, the frequency, the method used to measure it, etc. [23]. A theoretical determination of the dispersion relation $\omega = \omega(\alpha)$ is obtained from the solution of the problem of the stability of the tangential discontinuity [22] or the shear layer (see [12, 14], for instance). The mean value of the convective velocity of large-scale structures in the jets equals $U_c/U_\infty = 0.65$ [15]. We also take this value corresponding to the convective velocity of the most energetic vortices.

For $M_0 = 0$ a system of transcendental equations can be obtained to determine the natural vibrations frequencies of the cavity

$$\begin{aligned}(2/R)\,\mathrm{sh}\,\omega_r\cdot\cos\omega_i &= \cos(\theta-\alpha),\\ (2/R)\,\mathrm{ch}\,\omega_r\cdot\sin\omega_i &= \sin(\theta-\alpha).\end{aligned} \tag{3.8}$$

This system is solved numerically. Values of the natural frequencies are presented in Fig. 4 for positive ω_r in the form of solid lines. Different lines correspond to different vibrations modes, and dependences of the Strouhal number Sh_ℓ are superposed on the graph for five vibrations modes (k = 1-5). The computed values of Sh_ℓ lie somewhat above the experimental points. Let us note that stratification of the value of Sh_ℓ according to the vibrations modes is observed sufficiently clearly for both experimental and computed results. The amplitude distribution of the pressure fluctuations in the standing wave is given by (3.2) according to the model elucidated above. The amplitude distribution along the cavern bottom, measured

experimentally and presented in [7], has the same form characteristic for a standing wave.

If acoustic wave reflection from the forward endface of the cavity is neglected, i.e., it is considered that an acoustic wave being propagated in the negative x direction exists in the cavity, the value of the acoustic impedance is

$$Z = -1. \tag{3.9}$$

This corresponds to the zeroth approximation of the model [5] and the approximating relationships [11]. Using (3.9) is conjunction with (3.4) yields the dispersion equation for $M_0 = 0$

$$(R/2)\exp(-\omega_r)\exp[i(\theta - \alpha - \omega_i)] = 1.$$

The solution is found in the form

$$\omega_r = \ln(R/2),\ \alpha + \omega_i = 2\pi(k - 1/4),$$

where $\theta = -\pi/2$ is taken into account. The value of $F(\zeta)$ is taken from (3.7). Taking account of the parameters used to make the variables dimensionless, there is obtained for the natural frequencies

$$\mathrm{Sh}_l = (k - 1/4)/(U_\infty/a_0 + U_c/U_\infty), \tag{3.10}$$

which corresponds exactly to the zeroth approximation obtained in [5]. Values of Sh_ℓ calculated by means of (3.10) are superposed by dashes in Fig. 4 and differ inessentially from the values calculated by means of (3.8).

The author is grateful to V. V. Vedernikova for assistance in performing the experiments and carrying out the research.

LITERATURE CITED

1. V. N. Kudryavtsev, A. Ya. Cherkez, and V. A. Shilov, "Investigations of supersonic flow around two separating bodies," Izv. Akad. Nauk SSSR, Mekh. Zdidk. Gaza, No. 2 (1969).
2. V. S. Khlebnikov, "Investigation of the flow in front of a disc placed in the wake of a body in a supersonic flow," Trudy TsAGI, No. 1419 (1972).
3. P. K. Chang, Separation of Flow, Pergamon (1970).
4. W. Saroya, "Experimental investigations of fluctuations occurring in the flow around shallow channels," AIAA J., 15, No. 7 (1977).
5. A. N. Antonov, A. N. Vishnyakov, and S. P. Shalaev, "Experimental investigation of pressure fluctuations in a channel around which a subsonic or supersonic gas flows," Zh. Prikl. Mekh. Tekh. Fiz., No. 3 (1981).
6. S. A. Elder, "Self-excited depth-mode resonance for a wall-mounted cavity in turbulent flow," J. Acoust. Soc. Am., 64, No. 3 (1978).
7. H. H. Heller, D. G. Holmes, and E. E. Covert, "Flow induced pressure oscillations in shallow cavities," J. Sound Vibr., 18, Pt. 4 (1971).
8. M. G. Morozov, "Self-excitation of oscillations in supersonic separation flows," Inzh.-Fiz. Zh., 27, No. 5 (1974).
9. L. F. East, "Aerodynamically induced resonance in rectangular cavities," J. Sound Vibr., 3, No. 3 (1966).
10. J. E. Rossiter, "Wind-tunnel experiments on the flow over rectangular cavities at subsonic and transonic speeds," Aero. Res. Council, RM. No. 3438, London (1966).
11. V. L. Henke and J. G. Sheng, "Analysis of pressure fluctuations in an open cavity," AIAA J., 18, No. 8 (1980).
12. C. K. W. Tam and P. F. W. Block, "On the tones and pressure oscillations induced by flow over rectangular cavities," J. Fluid Mech., 89, Pt. 2 (1978).
13. L. S. Volovel'skii, V. D. Girgor'ev, V. I. Zapryagaev, et al., "Metrological investigations of the thermal wind tunnel T-333," Reports, Third All-Union School on Aerophysical Investigation Methods [in Russian], Novosibirsk (1982).
14. S. A. Gaponov and A. A. Maslov, Perturbation Development in Compressible Flows [in Russian], Nauka, Novosibirsk (1980).
15. A. Michalke and H. V. Fuchs, "On the turbulence and noise of an axisymmetric shear flow," J. Fluid Mech., 70, Pt. 1 (1975).
16. E. J. Skudrzyk, Foundations of Acoustics, Springer-Verlag (1972).
17. V. S. Avduevskii, V. K. Gretsov, and K. I. Medvedev, "Stability of flows with forward stall zones," Izv. Akad. Nauk SSSR, Mekh. Zhidk. Gaza, No. 1 (1972).

18. A. N. Antonov and V. K. Gretsov, "Investigation of the nonstationary separation supersonic flow around bodies," Izv. Akad. Nauk SSSR, Mekh. Zhidk. Gaza, No. 4 (1974).
19. V. N. Glaznev and V. S. Demin, "Semiempirical theory of discrete tone generation by a supersonic underexpanded jet impinging on an obstacle," Zh. Prikl. Mekh. Tekh. Fiz., No. 6 (1976).
20. B. V. Raushenbakh, Vibration Combustion [in Russian], GIFML, Moscow (1961).
21. B. V. Sobolev, "On the question of fluctuation measurements in jets," Vopr. Gazodin., Novosibirsk (1975).
22. T. Kh. Sedel'nikov, Self-Oscillatory Noise Formation in Gas Jet Escapes [in Russian], Nauka, Moscow (1971).
23. A. K. M. F. Hussein and A. R. Clark, "Determination of the statistical coupling between the dimensions and the convective velocity of turbulent structures in plane and circular jets," AIAA J., 19, No. 1 (1981).

THE ROLE OF THE FIRST AND SECOND MODES IN COMPRESSIBLE BOUNDARY-LAYER TRANSITION

V. I. Lysenko

UDC 532.526

At present there is no complete theory that can predict the transition location in a compressible boundary layer. In practice, however, the well-developed approximate methods based, as a rule, on linear stability theory are used (see, e.g., [1]). In the absence of information on the initial disturbance spectrum in the boundary layer (e.g., in flight tests) it is possible to use the (crude) e^n-method to locate transition. This method has been effective at subsonic speeds in "wind-tunnel" as well as flight tests including three-dimensional boundary layers (see, e.g., [2]). In this method the transition location is fixed when the disturbance amplitude ratio $A = Q/Q_0$ attains the value e^n (Q_0 is the disturbance amplitude at the lower branch of the neutral stability curve, Q is the current value of the amplitude, and n is specified) which is the amplification ratio in the unstable region. The transition Reynolds number determined in such a manner is an integral characteristic of the boundary-layer instability. It can be used to lucidly compare the contributions made by the first and the second modes to the growth of unstable disturbances in the boundary layer and investigate the influence of various factors on both the modes. A comparison of stability characteristics (growth rate, neutral curves, and transition Reynolds number) of the first and the second disturbance modes is the primary objective of the present paper.

1. The basis for this study is the program to compute disturbance amplification rate α_i in the boundary layer with heat transfer [3]. A detailed description of the computational technique to determine the stability characteristics is given in [1, 4].

Consider a compressible, heat conducting, two-dimensional boundary layer (see, e.g., [5] for the system of equations). Computationals are carried out for air flow on an impermeable surface with a specified wall temperature. Almost all computations are carried out for zero pressure gradient flow past a cone. The only exception was the study of the influence of pressure gradient on the amplification ratio.

The system of equations describing the flow in the boundary layer was transformed to a system of ordinary differential equations (for the flow with a pressure gradient local similarity was assumed [5]) which was then numerically integrated (see [1] for details). Numerical integration was used to determine the streamwise velocity and temperature distributions, their derivatives and the variation of viscosity across the boundary layer. These were required for the solution of the stability equations. In order to determine the amplification ratio the Dunn–Lin [6] approximation was used for the system of stability equations with boundary conditions: streamwise and normal velocity as well as temperature

Novosibirsk. Translated from Zhurnal Prikladnoi Mekhaniki i Tekhnicheskoi Fiziki, No. 6, pp. 58-62, November-December, 1985. Original article submitted January 2, 1985.